

## Far-Infrared Measurement of the Energy Gap of $V_3Si$ <sup>†</sup>

D. B. Tanner\* and A. J. Sievers

Laboratory of Atomic and Solid State Physics, Cornell University Ithaca, New York 14850

(Received 28 September 1972)

We have measured in the far infrared ( $2\text{--}70\text{ cm}^{-1}$ ) the difference between the surface impedances of normal and superconducting  $V_3Si$  at various temperatures. The radiation was transmitted through a nonresonant cavity containing several single-crystal slabs of  $V_3Si$  using a lamellar grating interferometer in conjunction with a  $^3He$ -cooled bolometer detector. A vacuum window isolated the detector from the nonresonant cavity. Temperature-dependence measurements have been made up to  $30^\circ K$  and no change in the surface impedance was observed near the martensitic phase transition at  $21^\circ K$ . There was a spread in the value of the energy gap, extending, at  $4.2^\circ K$ , from  $12\text{ cm}^{-1}$  ( $2\Delta_{\min} = 1.0kT_c$ ) to  $46\text{ cm}^{-1}$  ( $2\Delta_{\max} = 3.8kT_c$ ).

### I. INTRODUCTION

$V_3Si$  is one of a family of binary intermetallic compounds which have some of the highest superconducting transition temperatures yet known. These compounds have the form  $M_3Y$ , where  $M$  is a transition metal and  $Y$  is usually a semimetal or semiconductor. Certain of them, including  $V_3Si$ , undergo a cubic-to-tetragonal lattice-phase transition<sup>1</sup> at temperatures above the superconducting transition. The two temperatures in the case of  $V_3Si$  are  $T_m = 21^\circ K$  (for the lattice or martensitic transition) and  $T_c = 17.1^\circ K$  (for the superconducting transition).

Previous measurements of the energy gap of  $V_3Si$  and its sister compound  $Nb_3Sn$  have given varying results.<sup>2-5</sup> Values of the energy gap have varied from  $2\Delta = 1.0kT_c$  to  $2\Delta = 3.8kT_c$ . Tunneling measurements on single-crystal  $Nb_3Sn$  by Hoffstein and Cohen<sup>4</sup> showed an anisotropic gap, which depended on the direction of the tunneling current. The gap was a maximum in the  $[100]$  direction, with  $2\Delta = 2.8kT_c$ , and a minimum in the  $[111]$  direction, with  $2\Delta = 1.0kT_c$ .

### II. EXPERIMENTAL TECHNIQUES

The experiments were done in the cryostat shown in Fig. 1. The samples were single-crystal slabs of  $V_3Si$  which were grown in the MSC Materials Preparation facility at Cornell University. The boule was generally cylindrical and it was sliced lengthwise several times with a spark cutter. The resulting thin slabs had faces nearly parallel with the  $(210)$  crystal plane. These pieces were chemically polished with a 50-50 mixture of  $HF$  and  $HNO_3$  and four of them were glued to the cylinder walls of the nonresonant cavity. The specimens had a total exposed area of  $15\text{ cm}^2$ . The placement of two of the specimens is indicated in Fig. 1; the other two were on the sides of the cavity. A cross section of the cavity is shown in Fig. 1.

It is a right-circular cylinder, 1.5 cm in diameter and 4 cm long.

The incoming far-infrared radiation from a lamellar grating interferometer enters the cavity through a condensing cone on the cylinder wall. As calculated by Williamson's<sup>6</sup> equation, this cone demagnifies the radiation (reduces the diameter of the beam) from 1.27 to 0.5 cm and increases its half-angle (the maximum angle any ray makes with the axis of the light pipe) from  $18^\circ$  to  $90^\circ$ . Radiation leaves the small end of the cone with a  $2\pi$  solid angle, going into all parts of the cavity. Once inside the cavity, the radiation bounces around a few hundred times off the sample and finds

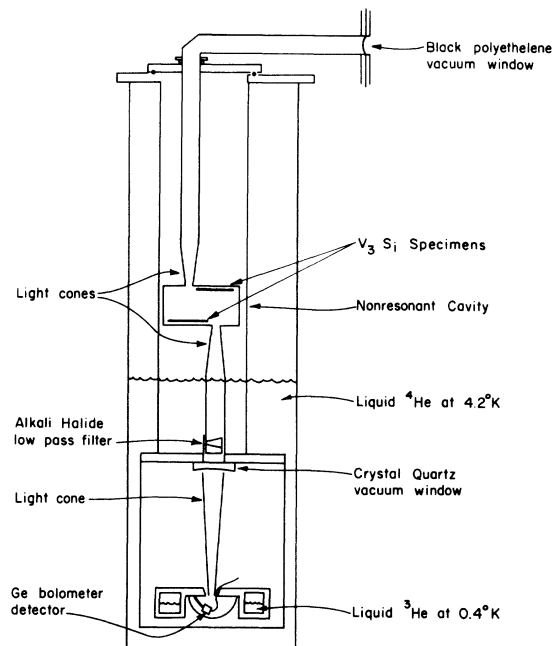


FIG. 1. Cryostat containing  $^3He$ -cooled bolometer and nonresonant cavity.

its way to the exit cone which converts it back to an  $18^\circ$  half-angle. From there it goes down a standard light pipe, through a quartz vacuum window to a pumped  $^3\text{He}$ -temperature bolometer detector.<sup>7</sup> A heater and carbon resistor are attached to the cavity, to allow the temperature to be adjusted and measured. Temperature isolation of the cavity from the detector was good enough that the cavity could be heated above  $30^\circ\text{K}$  without adversely affecting the detector. This cavity differs from those described by Richards and Tinkham<sup>8</sup> and by Leslie and Ginsburg<sup>9</sup> in this remote location of the detector.

The nonresonant cavity can be analyzed in terms of its quality factor  $Q$  as discussed by Lamb<sup>10</sup> or Townes and Schawlow.<sup>11</sup> This is defined as  $Q = 2\pi(\text{energy stored in cavity})/(\text{energy lost per cycle})$ . The energy transmitted through the cavity to the detector is proportional to  $Q$ . In this experiment, the transmission of the cavity was measured at two temperatures, one with the  $V_3Si$  superconducting and one with it normal and the ratio of these taken to eliminate any frequency dependence not due to the sample. The ratio of transmitted intensities is given by

$$\frac{I_S}{I_N} = \frac{Q_S}{Q_N} = \frac{3A + 16S(R_N/R_0)}{3A + 16S(R_S/R_0)},$$

where the subscripts  $N$  and  $S$  refer to the normal and superconducting states, respectively.  $A$  is the total area of the holes,  $S$  is the surface area

of the specimens,  $R_0$  is the impedance of free space ( $R_0 = 377 \Omega$ ), and  $R_N$  and  $R_S$  are the appropriate surface impedances of the specimen. The equation immediately above may be rewritten

$$\frac{R_N - R_S}{1 + \gamma(R_S/R_0)} = \frac{R_0}{\gamma} \left( \frac{I_S}{I_N} - 1 \right),$$

where  $\gamma = 16S/3A$ . If  $\gamma R_S/R_0 \ll 1$ , there is a simple relationship between the surface impedances in the normal and superconducting states and the measured intensities. In the configuration used in these experiments,  $\gamma = 200 \pm 10$ . At low frequencies ( $10 \text{ cm}^{-1}$ ),  $R_S \sim 0$  and the inequality is satisfied. At high frequencies ( $50 \text{ cm}^{-1}$ ),  $R_S \sim R_N \sim 10^{-3} R_0$  and  $\gamma R_S/R_0 \sim 0.2$ . Neglecting this term at these frequencies would decrease the value for  $R_N - R_S$  by about 20%. For the sake of simplicity, the function

$$\frac{R_N - R_S}{1 + \gamma R_S/R_0}$$

will be called "the surface-impedance difference" in the text of this paper.

### III. EXPERIMENTAL RESULTS

The difference in surface impedance between the normal and the superconducting states in  $\Omega$  as a function of frequency in  $\text{cm}^{-1}$  is shown in Fig. 2. The experimental data are shown as solid dots; a few have error bars on them. Resolution is  $1.5 \text{ cm}^{-1}$ . The superconducting data were taken at  $4.2^\circ\text{K}$  and the normal-state data at  $20^\circ\text{K}$ . The rise at the lowest frequencies is due to absorption in the normal metal, which increases

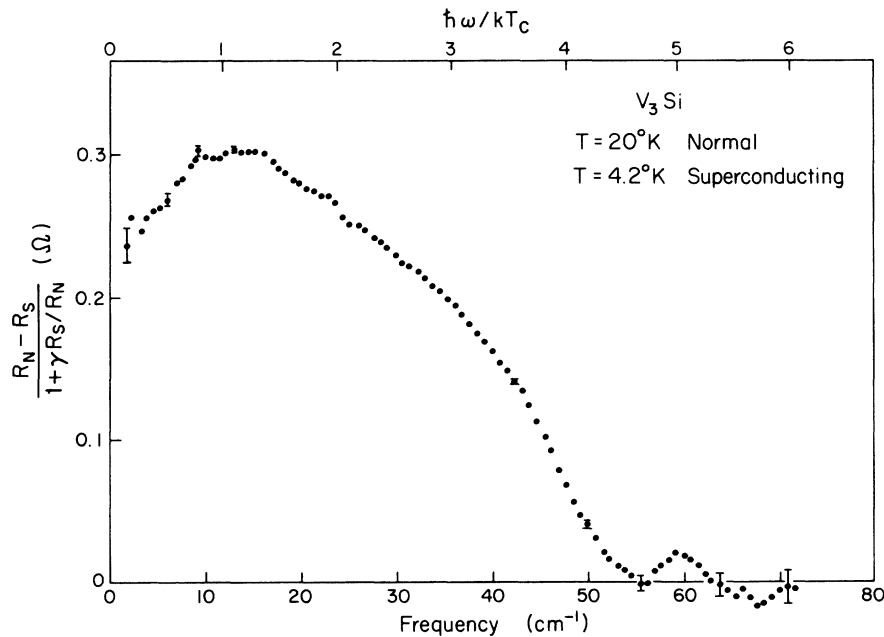


FIG. 2. Difference between normal and superconducting states surface impedance vs frequency for  $V_3Si$ .

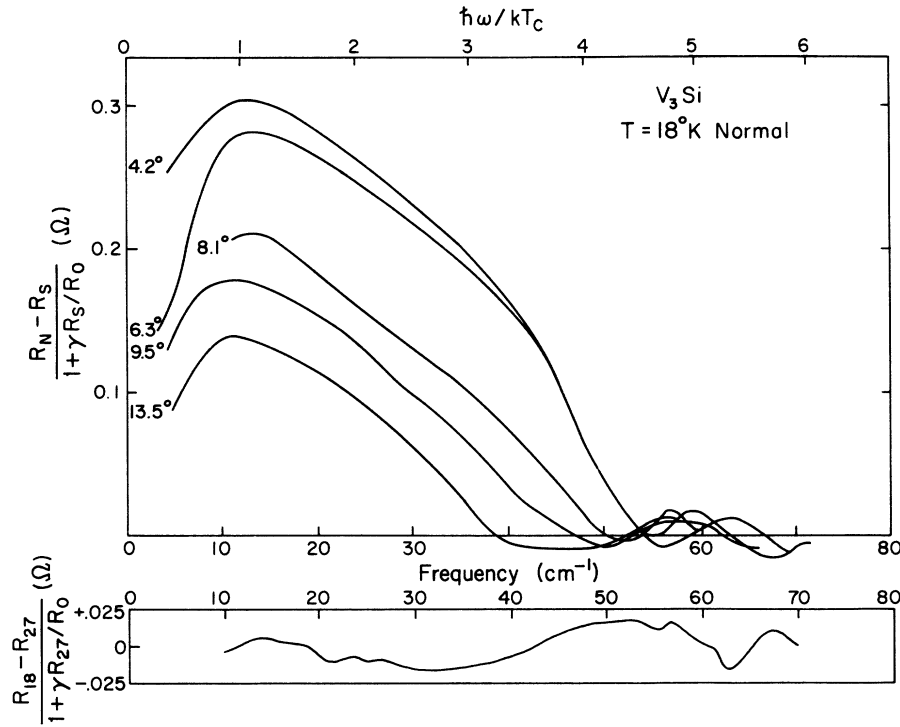


FIG. 3. Surface-impedance difference vs frequency for  $V_3Si$  at several temperatures.

with frequency. The peak at  $12\text{ cm}^{-1}$  ( $1.0kT_c$ ) indicates the frequency at which the superconductor begins to absorb; the surface impedance of the normal metal continues to rise, but that of the superconductor rises more steeply still, so that the

difference falls as the frequency increases. This fall attains its steepest slope at  $46\text{ cm}^{-1}$  ( $= 3.8kT_c$ ). At  $53\text{ cm}^{-1}$  ( $4.4kT_c$ ) the superconductor absorbs as strongly as the normal metal, and the difference continues near zero to our upper-frequency limit.

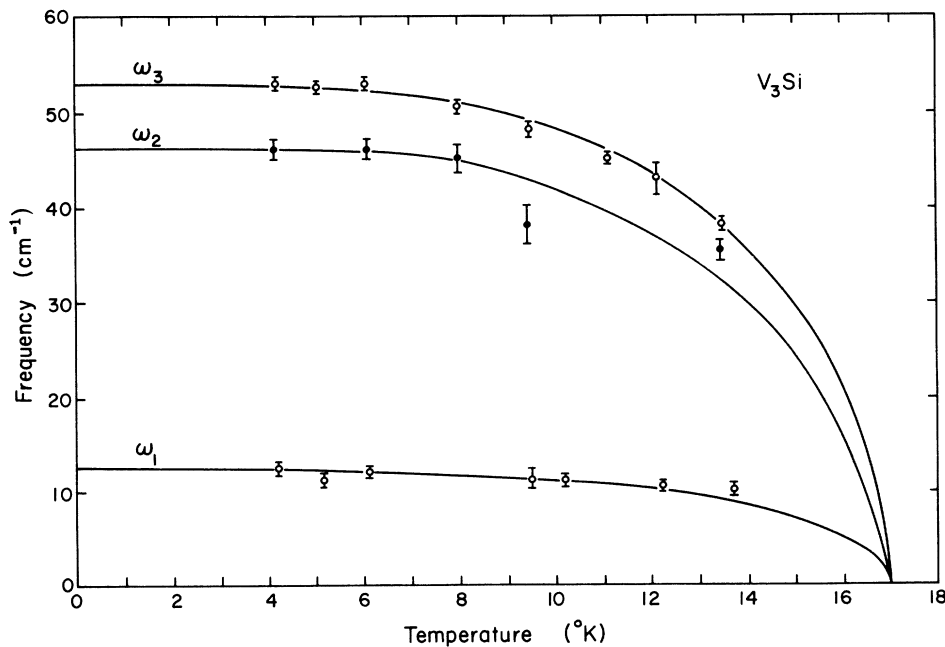


FIG. 4. Temperature dependence of the peak ( $\omega_1$ ), the point of maximum slope ( $\omega_2$ ), and the zero intercept ( $\omega_3$ ) of the impedance-difference curves. The points for  $\omega_2$  are shown as solid circles; the others are shown as open circles.

The absorption edge in superconductors has been discussed at length by Tinkham.<sup>12</sup> In isotropic superconductors, the surface-impedance difference is a maximum at the energy gap and falls to zero at a frequency somewhat above the gap. A calculation in the BCS theory<sup>9</sup> gives zero impedance difference at  $\hbar\omega \sim 2.2(2\Delta)$ , where  $2\Delta$  is the energy gap. The slope of the impedance difference is a maximum just above the gap at  $\hbar\omega \sim 1.3(2\Delta)$ . Measurements on the absorption edge show a much steeper edge. Recent experiments on lead by Brandli and Sievers<sup>13</sup> show the impedance difference to be zero at  $\hbar\omega \sim 1.3(2\Delta)$  and, to within the resolution, the maximum slope at  $\hbar\omega \sim 2\Delta$ . Similar measurements were reported earlier by Leslie and Ginsburg<sup>9</sup> and Richards and Tinkham.<sup>8</sup>

In the case of the present work, there is a range of values of the energy gap. The minimum is clearly at the peak in the curve of impedance difference:

$$2\Delta_{\min} = 1.0kT_c.$$

From the above discussion, we identify the maximum to be at the point of maximum slope in the impedance curve:

$$2\Delta_{\max} = 3.8kT_c.$$

The next figure (Fig. 3) shows the surface-impedance difference at various temperatures. As the temperature is increased, the height of the peak is reduced and shifts to lower frequencies. The zero impedance difference and the point of maximum slope also shift to lower frequencies, although the latter is difficult to see on this figure. The little box at the bottom of the figure shows the results when the metal is normal at both temperatures. The surface impedance at 27 °K differs from that at 18 °K by at most a small amount. Within the limits of the far-infrared sensitivity there is no evidence for a change in the

surface impedance at the martensitic phase transition.

In Fig. 4 is shown the temperature dependence of the three important frequencies. The upper curve is for the zero-impedance-difference intercept  $\omega_3$ , the middle curve for the maximum slope of the surface impedance  $\omega_2$ , and the lower curve for the peak  $\omega_1$ , where the superconductor begins to absorb. The solid lines show the BCS expression for the temperature dependence of the energy gap, scaled to go through  $T_c$  and the points at 4.2 °K.

#### IV. SUMMARY AND CONCLUSIONS

Measurements of the surface impedance as a function of far-infrared frequency at various temperatures on single-crystal  $V_3Si$  show a spread of values for the energy gap. The gap at 4.2 °K extends from  $2\Delta = 1.0kT_c$  to  $2\Delta = 3.8kT_c$ . These values take in the whole range of reported gap values from tunneling measurements in  $V_3Si$ . This spread is consistent with and can be explained by an anisotropic energy gap, as has been seen in  $Nb_3Sn$  in tunneling.<sup>4</sup> Both the upper and the lower value for the energy gap seem to follow the BCS form as a function of temperature and both have the same transition temperature.

A disadvantage of these experiments is that it is not possible to assign a particular gap value to a given crystal direction as was done in tunneling experiments.<sup>4</sup> A counter-balancing advantage is that the state of the surfaces is less important. In these extreme type-II superconductors the coherence length is much less than the penetration depth. In  $V_3Si$   $\xi_0 \sim 40 \text{ \AA}$ , while  $\lambda \sim 2000 \text{ \AA}$ . Tunneling measurements probe the material to the depth of the coherence length while far-infrared radiation goes into the penetration depth. It would be expected then that the far-infrared measurements would be much less affected by damage to the surface.

<sup>1</sup>Work supported by the U.S. Atomic Energy Commission under Contract No. AT(11-1)-3151, Technical Report No. COO-3151-11. Additional support was received from the National Science Foundation under Grant No. GH-33637 through the Cornell Materials Science Center, Report No. 1880.

<sup>\*</sup>Present address: Department of Physics, University of Pennsylvania, Philadelphia, Pa. 19174.

<sup>1</sup>B. W. Batterman and C. S. Barrett, Phys. Rev. Lett. **13**, 390 (1964).

<sup>2</sup>H. J. Levinstein and J. E. Kunzler, Phys. Lett. **20**, 581 (1966).

<sup>3</sup>J. J. Hauser, D. D. Bacon, and W. H. Haemmerle, Phys. Rev. **151**, 296 (1966).

<sup>4</sup>V. Hoffstein and R. W. Cohen, Phys. Lett. A **29**, 603 (1969).

<sup>5</sup>D. R. Bosomworth and G. W. Cullen, Phys. Rev. **160**, 346 (1967).

<sup>6</sup>D. E. Williamson, J. Opt. Soc. Am. **42**, 712 (1952).

<sup>7</sup>H. D. Drew and A. J. Sievers, Appl. Opt. **8**, 2067 (1969).

<sup>8</sup>P. L. Richards and M. Tinkham, Phys. Rev. **119**, 575 (1960).

<sup>9</sup>J. D. Leslie and D. M. Ginsburg, Phys. Rev. **133**, A362 (1964).

<sup>10</sup>W. E. Lamb, Phys. Rev. **70**, 308 (1946).

<sup>11</sup>C. H. Townes and A. L. Schawlow, *Microwave Spectroscopy*, (McGraw-Hill, New York, 1955), p. 391.

<sup>12</sup>M. Tinkham, in *Far-Infrared Properties of Solids*, edited by S. Mitra and S. Nudelman (Plenum, New York, 1970).

<sup>13</sup>G. Brandli and A. J. Sievers, Phys. Rev. B **5**, 3550 (1972).